

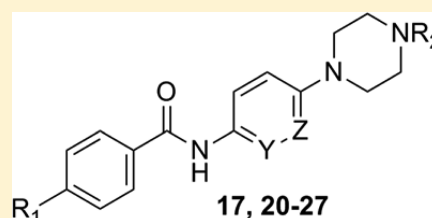
Towards Optimization of Arylamides As Novel, Potent, and Brain-Penetrant Antiprion Lead Compounds

Zhe Li,^{†,‡,||} Satish Rao,^{†,‡} Joel R. Gever,^{†,‡} Kartika Widjaja,[†] Stanley B. Prusiner,^{*,†,‡} and B. Michael Silber^{†,‡,§,⊥}[†]Institute for Neurodegenerative Diseases, [‡]Department of Neurology, [§]Department of Bioengineering and Therapeutic Sciences, University of California, San Francisco, California 94143, United States

S Supporting Information

ABSTRACT: The prion diseases caused by PrP^{Sc}, an alternatively folded form of the cellular prion protein (PrP^C), are rapidly progressive, fatal, and untreatable neurodegenerative disorders. We employed HTS ELISA assays to identify compounds that lower the level of PrP^{Sc} in prion-infected mouse neuroblastoma (ScN2a-cl3) cells and identified a series of arylamides. Structure–activity relationship (SAR) studies indicated that small amides with one aromatic or heteroaromatic ring on each side of the amide bond are of modest potency. Of note, benzamide (7), with an EC₅₀ of 2200 nM, was one of only a few arylamide hits with a piperazine group on its aniline moiety. The basic piperazine nitrogen can be protonated at physiologic pH, improving solubility, and therefore, we wanted to exploit this feature in our search for a drug candidate. An SAR campaign resulted in several key analogues, including a set with biaryl groups introduced on the carbonyl side for improved potency. Several of these biaryl analogues have submicromolar potency, with the most potent analogue 17 having an EC₅₀ = 22 nM. More importantly, 17 and several biaryl amides (20, 24, 26, and 27) were able to traverse the blood–brain barrier (BBB) and displayed excellent drug levels in the brains of mice following oral dosing. These biaryl amides may represent good starting points for further lead optimization for the identification of potential drug candidates for the treatment of prion diseases.

KEYWORDS: Neurodegenerative diseases, prion disease, Creutzfeldt–Jakob disease, amide, arylamide, SAR



Alzheimer's, Parkinson's, and Creutzfeldt–Jakob (CJD) diseases as well as the frontotemporal dementias are considered prion disorders.^{1,2} An expanding body of evidence argues that prions, or self-propagating proteins, cause many different neurodegenerative illnesses. The human prion diseases caused by the aberrant prion protein (PrP^{Sc}), which is formed posttranslationally from the cellular prion protein (PrP^C), include kuru, CJD, fatal insomnia, and Gerstmann–Sträussler–Scheinker disease.^{2,3} The conversion of the α -helical-rich PrP^C into an aberrant β -rich PrP^{Sc} conformer and accumulation of PrP^{Sc} are primary pathogenic events in prion disease.^{4,5} PrP^C-to-PrP^{Sc} conversion can occur spontaneously, result from inherited mutations in the gene encoding PrP^C, or be triggered by infection with exogenous PrP^{Sc}. Despite research efforts to find treatments for CJD, no therapy exists to date.^{6,7} While the exact mechanism of PrP^C misfolding is unclear, it is known that infectious prions can be transmitted and propagated in cell cultures such as murine neuroblastoma (ScN2a) cell lines.⁸ Screening efforts using these cell cultures have been carried out to discover antiprion compounds of different chemical classes.^{9–15} However, most of these antiprion leads are not drug-like and only demonstrate in vitro activity. To the best of our knowledge, Compd B, a phenyl hydrazone analogue, is the only small molecule reported to have efficacy in Rocky Mountain Laboratory (RML) prion-infected mouse models.¹⁶

As part of our ongoing medicinal chemistry program toward the screening and identification of potential therapeutics for

prion diseases, we focused on finding compounds that lower the levels of PrP^{Sc} in RML prion-infected neuroblastoma (ScN2a-cl3) cells.¹⁷ HTS of ~53 000 compounds resulted in the identification of 14 antiprion chemotypes, among which arylamides were the largest class of hits (Silber et al., in preparation). Herein, we report structure–activity relationship (SAR) analysis and preliminary lead optimization efforts aimed at improving the potency and physicochemical properties of the original arylamide hits. This effort led to several potent antiprion leads 17, 20, 24, 26, and 27, which also exhibited excellent in vitro metabolic stability and excellent in vivo brain exposure when dosed orally in mice.

To accompany all EC₅₀ measurements, compound toxicity toward ScN2a-cl3 cells was also evaluated using the fluorescent probe calcein-AM.¹³ Several brain-penetrant leads from the 2-aminothiazole (2-AMT) series, one of the 14 scaffolds, were identified after preliminary SAR studies.¹⁸ Despite this success, we discovered that the 2-AMTs suffered from generally poor aqueous solubility, resulting in the need to use PEG400 in our in vivo studies.¹⁹ To find superior leads, special attention was devoted to improving the physicochemical properties, especially solubility, of other chemical classes identified from our screening campaign. Arylamides represent the largest single

Received: December 17, 2012

Accepted: April 16, 2013

compound class from the ~53 000 compounds screened. Many of these simple aryl or heteroaryl amides (Supplementary Figure 1) displayed only moderate potency (EC_{50} = 1000–10 000 nM). Additionally, the aryl/heteroaryl rings of these amides form a highly conjugated system via the center amide bond and likely adopt a flat coplanar conformation, a structural feature often associated with poor solubility.^{20,21}

One amide, **7**, with moderate antiprion activity (EC_{50} = 2200 nM), has a basic *N*-benzylpiperazine substituent at the para position of its aniline moiety (Figure 1). The piperazine group

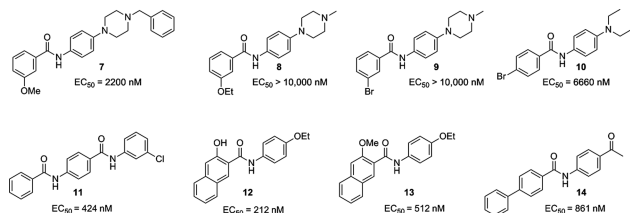


Figure 1. Selected arylamide hits and their antiprion potency.

has a $pK_a \approx 8.5$ and is protonated at physiologic pH, and thus confers superior solubility for the piperazine-containing molecule. We decided to explore the SAR on both sides of the amide bond of **7** with the initial goal of improving its potency (Figure 2). A closer survey of the initial actives showed

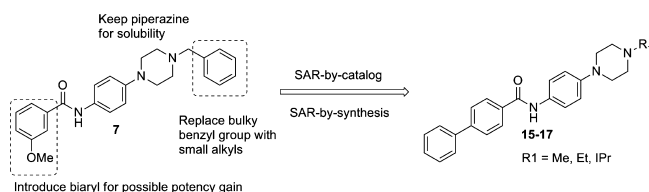


Figure 2. SAR strategy for HTS hit compound **7**.

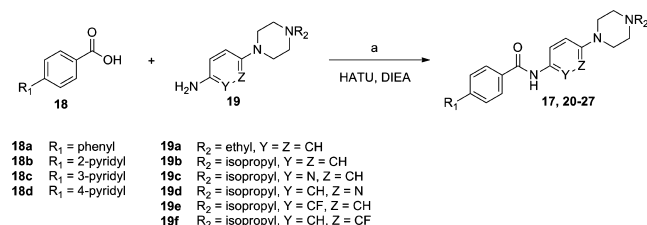
that amides with one aryl/heteroaryl group on both sides of the amide bond had only moderate antiprion potency (EC_{50} > 1000 nM; compounds **1–6** (Supplementary Figure 1) and **7–10** (Figure 1)). In contrast, amides with at least one biaryl in a fused or linear fashion displayed more potent antiprion activity (EC_{50} < 1000 nM; e.g., compounds **11–14**, Figure 1).

Hence, we decided to introduce a biaryl group to **7** on the carbonyl side and preserve the piperazine group on the aniline side of the amide for solubility considerations (Figure 2). In addition to introducing the biaryl moiety, we also sought to replace the bulky *N*-benzyl group on the piperazine with a smaller alkyl group, such as methyl or ethyl. The reasons for replacing the *N*-benzyl group are 2-fold. First, the *N*-benzyl group is flexible and likely adopts a noncoplanar conformation, which may be detrimental to antiprion potency (Silber et al., in preparation). Second, the replacement of the bulky *N*-benzyl with smaller alkyl groups should result in lead compounds with lower molecular weight.

Considering the 10-fold improvement in potency demonstrated by replacing the 4-ethoxy in **6** with a 4-phenyl to give the biaryl **14**, we decided to further explore this scaffold. In addition, the inactivity of both the 3-ethoxyphenyl amide (**8**) and the 3-bromophenyl amide (**9**) relative to the 4-bromophenyl amide (**10**) also suggested that substitution at the 4-position (i.e., 4-biphenyl analogues) might be favored over the corresponding 3-biphenyl congeners. Consistent with this SAR analysis, the *N*-methylated **15** was 4-fold more potent

than compound **7**, having an EC_{50} = 520 nM. The *N*-ethylpiperazine analogue (**16**) demonstrated further improvement in antiprion potency (EC_{50} = 221 nM). These results suggest that a larger *N*-alkyl group on the piperazine ring may be favorable for potency. The next analogue in the series, *N*-isopropylpiperazine analogue (**17**), was synthesized via standard amide coupling of commercially available 4-biphenylcarboxylic acid (**18a**) and 4-(4-isopropylpiperazin-1-yl)aniline (**19b**) (Scheme 1). As we had hoped, **17** showed further enhancement of antiprion activity, displaying an EC_{50} = 22 nM, a 100-fold increase over the original lead **7**.

Scheme 1. Synthesis of Biarylamides^a



^aReaction conditions: (a) HATU, DIEA, anhydrous DMF, rt, 12 h.

Given the promising potency of **17**, we sought to explore the SAR around the A- and C-rings (Figure 3; Table 1; **20–27**)

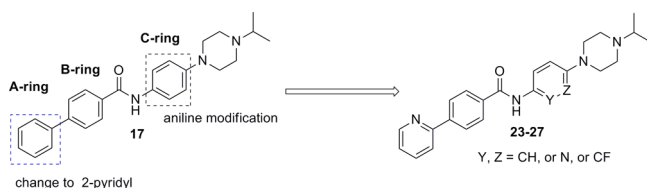


Figure 3. SAR strategy for modifying A-ring and C-ring of biphenyl lead **17**.

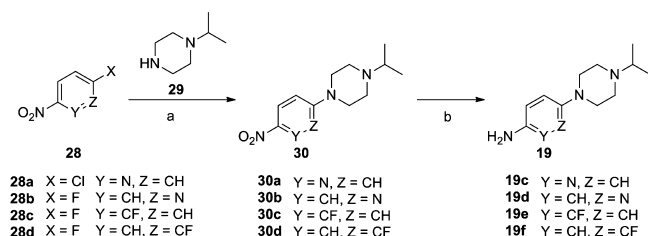
and initiated the synthesis of heterocyclic A-ring analogues in order to examine the effects of pyridyl biphenyls on antiprion potency. Three regioisomeric pyridyl congeners (**20–22**)

Table 1. Antiprion Potency (ELISA) and Cell Viability (Calcein AM) for Arylamide Analogues

	R ¹	Y	Z	R ²	ELISA $EC_{50} \pm SEM$ (nM)	calcein AM LD ₅₀ (nM)	n
15	phenyl	CH	CH	Me	520 ± 173	>5000	3
16	phenyl	CH	CH	Et	221 ± 95	>9000	3
17	phenyl	CH	CH	iPr	22 ± 4	>10000	4
20	2-pyridyl	CH	CH	Et	365 ± 70	>10000	3
21	3-pyridyl	CH	CH	Et	243 ± 29	>10000	3
22	4-pyridyl	CH	CH	Et	743 ± 25	>10000	3
23	2-pyridyl	CH	CH	iPr	165 ± 31	>10000	3
24	2-pyridyl	N	CH	iPr	348 ± 129	>10000	3
25	2-pyridyl	CH	N	iPr	677 ± 195	>10000	4
26	2-pyridyl	CF	CH	iPr	411 ± 123	>10000	3
27	2-pyridyl	CH	CF	iPr	334 ± 59	>10000	3

derived from **16** were synthesized according to Scheme 1 by direct amide couplings of the corresponding pyridylbenzoic acids (**18b–d**) and *N*-ethylpiperazineaniline (**19a**) (Supporting Information). All three pyridyl analogues (**20–22**) suffered up to a 3-fold potency loss compared to the parent biphenyl (**16**), suggesting that an electron-deficient group is not preferred at the terminal phenyl position. We also aimed to modify the C-ring of **17** because the electron-rich aniline moiety may be susceptible to oxidation mediated by CYP450 isozymes. Hence, reducing the electron density of the phenyl ring may alleviate the potential oxidation liability. Additionally, we also replaced the terminal phenyl of the biphenyl with a 2-pyridyl group in this C-ring pyridyl and fluoro-substituted C-ring series. To gain access to the key *N*-isopropylpiperazinylpyridinylamines (**19c** and **19d**) and fluoro *N*-isopropylpiperazinylaniline intermediates (**19e** and **19f**), appropriate halonitropyridines (**28a** and **28b**) or difluoronitrobenzenes (**28c** and **28d**) were reacted first with *N*-isopropylpiperazine (**29**) to give the corresponding *N*-isopropyl-4-(nitropyridinyl)piperazines (**30a** and **30b**) or *N*-(fluoro,nitrophenyl)-4-isopropylpiperazines (**30c** and **30d**) (Scheme 2). The nitro group (**30a–d**) was then selectively

Scheme 2. Synthesis of **19c–f**^a



^aReaction conditions: (a) CH₃CN, reflux, 5 h (for **30a** and **30b**) or K₂CO₃, HMPA, rt, 2 d (for **30c** and **30d**); (b) Pd/C, H₂, MeOH, rt, 12 h.

reduced to the corresponding amines **19c–f** by catalytic hydrogenation over palladium carbon in methanol. Finally, amide coupling of amines **19b–f** with [1,1'-biphenyl]-4-carboxylic acid (**18a**) or 4-(pyridin-2-yl)benzoic acid (**18b**) furnished the C-ring-modified products **24–27** (see Supporting Information). Unfortunately, these analogues showed much reduced antiprion potency, with their EC₅₀ values at least 15-fold greater than the parent biphenyl analogue **17** (Table 1).

As a prelude to in vivo efficacy studies, we performed in vivo mouse PK studies on the most active compounds in the series

to evaluate their PK profile and blood–brain barrier (BBB) permeability, thus assessing their potential as CNS drugs. We administered 8 compounds (**16**, **17**, **20**, **21**, **23**, **24**, **26**, and **27**) to mice, utilizing an abbreviated study protocol to obtain key parameters such as C_{max} and AUC in the brain, important criteria for initial compound selection and prioritization for efficacy studies. In general, for our single-dose PK studies, 10 mg/kg of each compound was administered by oral gavage. Brain and plasma concentration were measured at 0.5, 2, 4, and 6 h after administration. The C_{max} and AUC from time zero to 6 h (AUC_{0–6h}) for both brain and plasma were obtained (Table 2). To further aid compound prioritization, in vitro microsomal stability studies were also conducted using a standard protocol.

For biphenyl analogues, both the *N*-ethyl **16** (EC₅₀ = 221 nM) and the *N*-isopropyl **17** (EC₅₀ = 22 nM) displayed high concentrations in brain, with **16** having 3-fold higher exposure (C_{max} and AUC) than **17**. Because the *N*-isopropyl congener **17** is more stable (*t*_{1/2} > 60 min) in mouse hepatic microsomes than the smaller *N*-ethyl analogue **16** (*t*_{1/2} = 19.0 min), the lower brain exposure of **17** is likely caused by an absorption and/or permeability difference between the two congeners. Despite its lower brain exposure, **17** possesses higher C_{max}/EC₅₀ and AUC/EC₅₀ ratios than **16** due to its superior potency. More importantly, both analogues displayed at least 10-fold higher concentrations in brain than in plasma, typical of an effective CNS drug. An intriguing difference was found between the two close analogues **20** and **21**; the 2-pyridyl congener **20** had much higher brain exposure (>4-fold C_{max} and >7-fold AUC) than the 3-pyridyl congener **21**. Considering both analogues had similar stability in mouse hepatic microsomal preparations (*t*_{1/2} = 27.0 min for **20** and *t*_{1/2} = 29.2 min for **21**) (Table 2), this brain exposure difference may be due to absorption differences. Surprisingly, while the terminal 2-pyridyl biphenyl analogue (A-ring analogue) **23** exhibited much lower brain exposure than either **16** or **20**, it had superior hepatic mouse microsomal stability (*t*_{1/2} > 60 min); the reduced brain exposure may be due to poor BBB permeability and/or poor dissolution of compound **23**.

In summary, we have optimized a series of benzamides, typified by **7** with moderate antiprion potency (EC₅₀ = 2200 nM), to a series of potent biaryl amide leads, one (**17**) having an EC₅₀ of 22 nM. Additionally, several compounds (e.g., **17**, **24**, **26**, and **27**) demonstrated excellent metabolic stability in hepatic microsomal preparations, superior in vivo brain exposure, and highly favorable brain-to-plasma drug ratios. These piperazine-bearing biaryl amides represent an exciting

Table 2. In vivo Pharmacokinetic Parameters (Single Oral Dose of 10 mg/kg) and in vitro Microsomal Stability for Arylamide Analogues

compd	brain exposure		plasma exposure		microsomal stability	
	C _{max} (μM)	AUC (μM·h)	C _{max} (μM)	AUC (μM·h)	<i>t</i> _{1/2} in min (% remaining after 60 min incubation)	
					mouse	human
16	7.95 ± 2.40	25.4 ± 6.23	0.37 ± 0.20	1.09 ± 0.40	19.0 (12)	>60 (66)
17	2.52 ± 0.26	7.48 ± 0.77	0.27 ± 0.01	0.97 ± 0.03	>60 (51)	>60 (64)
20	6.23 ± 0.43	24.2 ± 4.39	0.28 ± 0.03	1.05 ± 0.21	27.0 (23)	>60 (50)
21	1.44 ± 0.13	3.32 ± 0.05	0.21 ± 0.02	0.25 ± 0.03	29.2 (24)	>60 (53)
23	0.09 ± 0.05	0.28 ± 0.11	0.32 ± 0.05	1.20 ± 0.16	>60 (61)	>60 (77)
24	6.00 ± 0.75	22.3 ± 1.20	0.34 ± 0.18	1.26 ± 0.46	>60 (57)	>60 (71)
26	17.3 ± 1.18	39.8 ± 9.84	0.65 ± 0.07	1.46 ± 0.00	57.3 (48)	>60 (76)
27	6.75 ± 0.95	28.7 ± 7.43	0.46 ± 0.04	2.28 ± 0.09	>60 (58)	>60 (83)

new class of antiprion compounds that warrant further studies in RML- and CJD-infected prion models.

■ ASSOCIATED CONTENT

● Supporting Information

Experimental and analytical data for compounds **17**, **20–27**, and **30a–d** and intermediates **19c–f**; biological methods; Supporting Figure 1. This material is available free of charge via the Internet at <http://pubs.acs.org>.

■ AUTHOR INFORMATION

Corresponding Author

*(S.B.P.) Phone: (415) 476-4482. Fax: (415) 476-8386. E-mail: stanley@ind.ucsf.edu.

Present Addresses

^{||}Global Blood Therapeutics, Inc., South San Francisco, California 94080, United States.

[†]ELMEDTECH, LLC, San Francisco, California 94123, United States.

Author Contributions

All authors have given approval to the final version of this manuscript.

Funding

This work was funded by grants from the NIH (AG021601, AG031220, AG002132, and AG010770) and by gifts from the Sherman Fairchild, Larry L. Hillblom, Rainwater Charitable, and Lincy foundations as well as from the Fight for Mike Homer Program, Robert Galvin, and Mary Jane Brinton.

Notes

The authors declare no competing financial interest.

■ ACKNOWLEDGMENTS

We thank Mr. Phillip Benner for preparing the animal dosing solution and collecting samples for PK studies; Ms. Priya Jaishankar for experimental assistance; Dr. Kurt Giles and the staff of the Hunter's Point animal facility for overseeing animal studies; Dr. Adam Renslo for helpful discussions; Dr. John Nuss for reviewing the manuscript; and Ms. Hang Nguyen for editorial assistance.

■ ABBREVIATIONS

2-AMT, 2-aminothiazole; CJD, Creutzfeldt–Jakob disease; DIEA, diisopropylethylamine; HATU, 2-(1*H*-7-azabenzotriazol-1-yl)-1,1,3,3-tetramethyluronium hexafluorophosphate; PrP^{Sc}, pathogenic isoform of the prion protein; RML, Rocky Mountain Laboratory; ScN2a-cl3, murine neuroblastoma clone3 cells

■ REFERENCES

- (1) Jucker, M.; Walker, L. C. Pathogenic protein seeding in Alzheimer disease and other neurodegenerative disorders. *Ann. Neurol.* **2011**, *70*, 532–540.
- (2) Prusiner, S. B. A unifying role for prions in neurodegenerative diseases. *Science* **2012**, *336*, 1511–1513.
- (3) Aguzzi, A.; Sigurdson, C.; Heikenwaelder, M. Molecular mechanisms of prion pathogenesis. *Annu. Rev. Pathol.* **2008**, *3*, 11–40.
- (4) Pan, K.-M.; Baldwin, M.; Nguyen, J.; Gasset, M.; Serban, A.; Groth, D.; Mehlhorn, I.; Huang, Z.; Fletterick, R. J.; Cohen, F. E.; Prusiner, S. B. Conversion of α -helices into β -sheets features in the formation of the scrapie prion proteins. *Proc. Natl. Acad. Sci. U.S.A.* **1993**, *90*, 10962–10966.
- (5) Prusiner, S. B. Shattuck Lecture: Neurodegenerative diseases and prions. *N. Engl. J. Med.* **2001**, *344*, 1516–1526.

- (6) Trevitt, C. R.; Collinge, J. A systematic review of prion therapeutics in experimental models. *Brain* **2006**, *129*, 2241–2265.
- (7) Sim, V. L.; Caughey, B. Recent advances in prion chemotherapeutics. *Infect. Disord.: Drug Targets* **2009**, *9*, 81–91.
- (8) Nishida, N.; Harris, D. A.; Vilette, D.; Laude, H.; Frobert, Y.; Grassi, J.; Casanova, D.; Milhavet, O.; Lehmann, S. Successful transmission of three mouse-adapted scrapie strains to murine neuroblastoma cell lines overexpressing wild-type mouse prion protein. *J. Virol.* **2000**, *74* (1), 320–325.
- (9) Caspi, S.; Sasson, S. B.; Taraboulos, A.; Gabizon, R. The anti-prion activity of Congo red. Putative mechanism. *J. Biol. Chem.* **1998**, *273* (6), 3484–3489.
- (10) Dollinger, S.; Lober, S.; Klingenstein, R.; Korth, C.; Gmeiner, P. A chimeric ligand approach leading to potent antiprion active acridine derivatives: design, synthesis, and biological investigations. *J. Med. Chem.* **2006**, *49*, 6591–6595.
- (11) Heal, W.; Thompson, M. J.; Mutter, R.; Cope, H.; Louth, J. C.; Chen, B. Library synthesis and screening: 2,4-diphenylthiazoles and 2,4-diphenyloxazoles as potential novel prion disease therapeutics. *J. Med. Chem.* **2007**, *50*, 1347–1353.
- (12) Kimata, A.; Nakagawa, H.; Ohshima, R.; Fukuchi, T.; Ohta, S.; Doh-ura, K.; Suzuki, T.; Miyata, N. New series of antiprion compounds: pyrazolone derivatives have the potent activity of inhibiting protease-resistant prion protein accumulation. *J. Med. Chem.* **2007**, *50*, 5053–5056.
- (13) May, B. C. H.; Zorn, J. A.; Witkop, J.; Sherrill, J.; Wallace, A. C.; Legname, G.; Prusiner, S. B.; Cohen, F. E. Structure–activity relationship study of prion inhibition by 2-aminopyridine-3,5-dicarbonitrile-based compounds: Parallel synthesis, bioactivity and in vitro pharmacokinetics. *J. Med. Chem.* **2007**, *50*, 65–73.
- (14) Thompson, M. J.; Borsenberger, V.; Louth, J. C.; Judd, K. E.; Chen, B. Design, synthesis, and structure–activity relationship of indole-3-glyoxylamide libraries possessing highly potent activity in a cell line model of prion disease. *J. Med. Chem.* **2009**, *52*, 7503–7511.
- (15) Thompson, M. J.; Louth, J. C.; Ferrara, S.; Jackson, M. P.; Sorrell, F. J.; Cochrane, E. J.; Gevers, J.; Baxendale, S.; Silber, B. M.; Roehl, H. H.; Chen, B. Discovery of 6-substituted indole-3-glyoxylamides as lead antiprion agents with enhanced cell line activity, improved microsomal stability and low toxicity. *Eur. J. Med. Chem.* **2011**, *46*, 4125–4132.
- (16) Kawasaki, Y.; Kawagoe, K.; Chen, C. J.; Teruya, K.; Sakasagawa, Y.; Doh-ura, K. Orally administered amyloidophilic compound is effective in prolonging the incubation periods of animals cerebrally infected with prion diseases in a prion strain-dependent manner. *J. Virol.* **2007**, *81*, 12889–12898.
- (17) Ghaemmaghami, S.; May, B. C. H.; Renslo, A. R.; Prusiner, S. B. Discovery of 2-aminothiazoles as potent antiprion compounds. *J. Virol.* **2010**, *84*, 3408–3412.
- (18) Gallardo-Godoy, A.; Gevers, J.; Fife, K. L.; Silber, B. M.; Prusiner, S. B.; Renslo, A. R. 2-Aminothiazoles as therapeutic leads for prion diseases. *J. Med. Chem.* **2011**, *54*, 1010–1021.
- (19) Silber, B. M.; Rao, S.; Fife, K. L.; Gallardo-Godoy, A.; Renslo, A. R.; Dalvie, D. K.; Giles, K.; Freyman, Y.; Elepano, M.; Gevers, J. R.; Li, Z.; Jacobson, M. P.; Huang, Y.; Benet, L. Z.; Prusiner, S. B. Pharmacokinetics and metabolism of 2-aminothiazoles with antiprion activity in mice. *Pharm. Res.* **2013**, *30*, 932–950.
- (20) Ishikawa, M.; Hashimoto, Y. Improvement in aqueous solubility in small molecule drug discovery programs by disruption of molecular planarity and symmetry. *J. Med. Chem.* **2011**, *54*, 1539–1554.
- (21) Lovering, F.; Bikker, J.; Humblet, C. Escape from flatland: increasing saturation as an approach to improving clinical success. *J. Med. Chem.* **2009**, *52*, 6752–6756.